Entropy production in photovoltaic-thermoelectric nanodevices from the non-equilibrium Green's function formalism

Fabienne Michelini, Adeline Crépieux, Katawoura Beltako

Entropy production in photovoltaic-thermoelectric nanodevices from the non-equilibrium Green's function formalism

Fabienne Michelini[1], **Adeline Crépieux**[2] **and Katawoura Beltako**[1]

[1] Aix Marseille Univ, Univ Toulon, CNRS, IM2NP, Marseille, France
[2] Aix Marseille Univ, Université de Toulon, CNRS, CPT, Marseille, France

E-mail: fabienne.michelini@im2np.fr

Abstract

We discuss some thermodynamic aspects of energy conversion in electronic nanosystems able to convert light energy into electrical or/and thermal energy using the non-equilibrium Green's function formalism. In a first part, we derive the photon energy and particle currents inside a nanosystem interacting with light and in contact with two electron reservoirs at different temperatures. Energy conservation is verified, and radiation laws are discussed from electron non-equilibrium Green's functions. We further use the photon currents to formulate the rate of entropy production for steady-state nanosystems, and we recast this rate in terms of efficiency for specific photovoltaic-thermoelectric nanodevices. In a second part, a quantum dot based nanojunction is closely examined using a two-level model. We show analytically that the rate of entropy production is always positive, but we find numerically that it can reach negative values when the derived particule and energy currents are empirically modified as it is usually done for modeling realistic photovoltaic systems.

Keywords: radiation laws, quantum thermodynamics, quantum dots, photovoltaics, non-equilibrium green's functions

1. Introduction

Nanoscale structures still reveals new insights and potential applications which alter our vision of technology. Device-integrated nanostructures fundamentally change the transport properties of electrons through quantum effects like tunneling, confinement or entanglement. As a result, many-body quantum methodologies are developing for practical purposes, such as for modeling electronic devices, like transistors [1], and more recently energy conversion systems like photovoltaics [2, 3], optomechanics [4] or thermoelectrics [5, 6]. The formalism of non-equilibrium Green's function (NEGFs) is one of the most convenient methodologies to deal with particle and energy transport in open interacting systems [7]. Quantum master equations are rather suited for weak coupling to electron reservoirs [8], or for optically driven systems. Quantum cascade laser simulations are also carried out from NEGF formalism [9]. In quantum thermodynamics [10, 11], including thermoelectricity, NEGF methodology permits to develop fundamental studies on time-resolved conversion [12–14], effects of electron-electron interaction [15, 16], fundamental laws [17–19], and potential new paradigms [20, 21]. In quantum optoelectronics [22] and photovoltaics [23], the need to improve our understanding of innovative

nanotechnology-enabled concepts accelerates the development of NEGF-based approaches [24, 25]. Another possible application follows the idea of cogeneration, which combines outputted energy forms from a single sustainable energy source, like the simultaneous production of electrical and thermal energies from a single light source. At the commercial level, stacked photovoltaic-thermoelectric macroscopic modules have been created and analyzed [26, 27]. Perovskites show potentials both as photovoltaics [28] and thermoelectrics [29], which suggests that a combined energy conversion with these materials could be a success [30]. Nanoscale architectures have been theoretically proposed for cooling using a photon source [31–34], and for joint cooling and electrical energy production [35]. These proposals address the idea of cogeneration inside a unique nanoscale module, which requires a deeper look at the quantum aspects of the energy conversion involving light-matter interaction. This perspective is related to the thermodynamics of light [36] which has naturally emerged in photovoltaics regarding the photon source as a thermal bath [37], but also the contact as a thermoelectric junction between the absorber and the lead [38, 39]. In these nanoscale proposals, reversibility remains a cornerstone as it defines the maximal efficiency, and the efficiency at maximum power achievable [40]: the entropy production rate is a crucial ingredient of device working. However, entropy cannot be represented by a Hermitian operator in quantum physics.

In this work, we derive the photon energy and particle currents in open nanosystems interacting with light using the framework of NEGFs. The Hamiltonian model is introduced in section 2, and the main steps and consequences of the derivation are given in section 3. This allows to calculate the entropy current flowing from the electron and photon reservoirs to the absorbing region of the device in section 4: we reshape and discuss the entropy production in terms of efficiencies for photovoltaic-thermoelectric nanodevices. In section 5, we finally examine a quantum-dot based architecture illuminated with a monochromatic radiation. Using a two-level model, we show that the entropy production rate is always positive at any coupling to electron reservoirs as long as one considers the same radiation properties for the spontaneous emission. However, we find that the entropy production rate can reach negative values if modifications are made inside the approach, as it is usually done for photovoltaic device simulations.

2. Hamiltonian model

The Hamiltonian of a quantum nanosystem in contact with electronic reservoirs and interacting with light reads

$$H = H_0 + H_T + H_{\rm int} + H_L + H_R + H_\gamma, \tag{1}$$

where

$$H_0 = \sum_n \epsilon_n d_n^\dagger d_n, \tag{2a}$$

$$H_T = \sum_{\alpha=L,R} \sum_{n\mathbf{k}} V_{\alpha n\mathbf{k}} c_{\alpha n\mathbf{k}}^\dagger d_n + \text{h.c.}, \tag{2b}$$

$$H_{\rm int} = \sum_{nm,\zeta\mathbf{q}} M_{nm,\zeta\mathbf{q}} d_n^\dagger d_m A_{\zeta\mathbf{q}}, \tag{2c}$$

$$H_{\alpha\in\{L,R\}} = \sum_{n\mathbf{k}} \epsilon_{\alpha n\mathbf{k}} c_{\alpha n\mathbf{k}}^\dagger c_{\alpha n\mathbf{k}}, \tag{2d}$$

$$H_\gamma = \sum_{\zeta\mathbf{q}} \hbar\omega_{\zeta\mathbf{q}} \left[a_{\zeta\mathbf{q}}^\dagger a_{\zeta\mathbf{q}} + \frac{1}{2} \right]. \tag{2e}$$

Subscript 0 stands for the non-interacting and isolated nanosystem, T for the transfer to the electron reservoirs, *int* for the interaction with light, α for the the left (L) and right (R) electron reservoirs, and γ for the photon bath. These expressions use the electron creation (annihilation) operators, $d_n^\dagger$ (d_n) in the central region and $c_{\alpha n\mathbf{k}}^\dagger$ ($c_{\alpha n\mathbf{k}}$) in the electron reservoirs. On the other side, $a_{\zeta\mathbf{q}}^\dagger$ ($a_{\zeta\mathbf{q}}$) and $A_{\zeta\mathbf{q}} = a_{\zeta\mathbf{q}} + a_{\zeta-\mathbf{q}}^\dagger$ are photon operators of the photon bath, with $\mathbf{q}$ the wave vector of the radiation, and ζ one of the two directions of polarization perpendicular to the propagation. The interacting central region is coupled to the electron reservoirs via parameters $V_{\alpha n\mathbf{k}}$ while it is coupled to the light radiation via parameters $M_{nm,\zeta\mathbf{q}}$. Usually, calculation for optoelectronics relies on the dipole approximation: $\mathbf{q}\cdot\mathbf{r} \ll 1$ where $\mathbf{r}$ is the spatial coordinate [41].

We introduce the notations used in this paper: $I_\beta^E = -\langle \dot{H}_\beta \rangle$ the energy current, $I_\beta = -\langle \dot{N}_\beta \rangle$ with $N_{\beta\in\{L,R\}} = \sum_{n\mathbf{k}} c_{\beta n\mathbf{k}}^\dagger c_{\beta n\mathbf{k}}$ and $N_\gamma = \sum_{\zeta\mathbf{q}} a_{\zeta\mathbf{q}}^\dagger a_{\zeta\mathbf{q}}$ the particle current, and finally $I_\beta^h = -\langle \dot{H}_\beta \rangle + \mu_\beta \langle \dot{N}_\beta \rangle = I_\beta^E - \mu_\beta I_\beta^p$ for the heat current [12], where μ_β is the (electro)chemical potential of reservoir β. In the case of electron reservoirs, we will also use $I_{\beta\in L,R}^e$ for the electrical current. All currents are flowing from the $\beta \in L, R, \gamma$ reservoir to the central region.

3. Photon currents

3.1. Photon energy current

We derived the formal expression of the photon energy current $I_\gamma^E(t) = -\langle \dot{H}_\gamma \rangle(t)$ inside an optoelectronic device following the first order Born approximation within the Keldysh formalism [42, 43]. From the Heisenberg equation $\dot{H}_\gamma = -\frac{i}{\hbar}[H_\gamma, H]$, the energy current can be expressed in terms of expectation values on mixed operators which combine electron and photon operators

$$I_\gamma^E(t) = \frac{1}{\hbar} \,\text{Re} \sum_{\zeta\mathbf{q}} \hbar\omega_{\zeta\mathbf{q}} \mathbf{M}_{\zeta\mathbf{q}} \mathfrak{B}_{\zeta\mathbf{q}}^<(t,t), \tag{3}$$

where $\mathfrak{B}_{mn,\zeta\mathbf{q}}^<(t,t) = \mathrm{i}\langle d_n^\dagger(t) d_m(t) B_{\zeta\mathbf{q}}(t) \rangle$ with $B_{\zeta\mathbf{q}}(t) = a_{\zeta\mathbf{q}}(t) - a_{\zeta-\mathbf{q}}^\dagger(t)$. Here we use matrix forms to encode level and/or eventual space-discretization indices. In the framework of the Keldysh formalism, we sought the expression of the contour ordered mixed Green's function

$$\mathfrak{B}_{mn,\zeta\mathbf{q}}^t(\tau,\tau') = -\mathrm{i}\langle T d_m(\tau) d_n^\dagger(\tau') B_{\zeta\mathbf{q}}(\tau) \rangle, \tag{4}$$

where T is the time-ordering operator. The main steps of the derivation follow the first order Born approximation [43], which consists in switching to the interaction picture, developing the time evolution operator up to the second order in the electron-boson interaction parameter, using Wick's theorem[3], verifying the cancellation of the disconnected graphs, including higher order contributions with self-consistency, and finally performing the Langreth's rules for the analytic continuation. We thus obtain

$$\sum_{\zeta\mathbf{q}} \hbar\omega_{\zeta\mathbf{q}} \mathbf{M}_{\zeta\mathbf{q}} \mathfrak{B}^{<}_{\zeta\mathbf{q}}(\tau,\tau') = \mathrm{Tr} \int \mathrm{d}\tau_1 \Xi^{t}_{\gamma}(\tau,\tau_1)\, \mathbf{G}^{t}(\tau_1,\tau'), \tag{5}$$

with

$$\Xi^{t}_{\gamma}(\tau,\tau_1) = \sum_{\zeta\mathbf{q}} \hbar\omega_{\zeta\mathbf{q}} \mathbf{M}_{\zeta\mathbf{q}} \mathbf{G}^{t}(\tau,\tau_1) \widetilde{D}^{0t}_{\zeta\mathbf{q}}(\tau,\tau_1) \mathbf{M}_{\zeta\mathbf{q}}. \tag{6}$$

The expression of $\mathfrak{B}^{<}_{mn,\zeta\mathbf{q}}(t,t)$ is then deduced from the Langreth's rules, which finally provides the photon energy current from equation (3),

$$I^{E}_{\gamma}(t) = \frac{1}{\hbar} \mathrm{Re}\,\mathrm{Tr} \int \mathrm{d}t_1 [\mathbf{G}^{r}(t,t_1)\Xi^{<}_{\gamma}(t_1,t) + \mathbf{G}^{<}(t,t_1)\Xi^{a}_{\gamma}(t_1,t)]. \tag{7}$$

These expressions use the standard Green's functions for the electrons inside the central region $\mathbf{G}^{t}(\tau,\tau')$, defined as $G^{t}_{nm}(\tau,\tau') = -\mathrm{i}\langle T d_n(\tau) d^{\dagger}_m(\tau')\rangle$. On the other side, we introduce the photon Green's function $\widetilde{D}^{0t}_{\zeta\mathbf{q}}(\tau,\tau_1) = -\mathrm{i}\langle T B_{\zeta\mathbf{q}}(\tau) A_{\zeta\mathbf{q}}(\tau_1)\rangle$. Function $\widetilde{D}^{0t}_{\zeta\mathbf{q}}(\tau,\tau_1)$ differs in a negative sign from $D^{0t}_{\zeta\mathbf{q}}(\tau,\tau_1) = -\mathrm{i}\langle T A_{\zeta\mathbf{q}}(t) A_{\zeta\mathbf{q}}(\tau_1)\rangle$ which appears in the derivation of the Dyson's equation for an electron interacting with bosons [43].

For steady-state devices, we obtain

$$I^{E}_{\gamma} = \frac{1}{\hbar} \mathrm{Re}\,\mathrm{Tr} \int \frac{\mathrm{d}\epsilon}{2\pi} [\mathbf{G}^{r}\Xi^{<}_{\gamma} + \mathbf{G}^{<}\Xi^{a}_{\gamma}](\epsilon), \tag{8}$$

where

$$\Xi^{\lessgtr}_{\gamma}(\epsilon) = \sum_{\zeta\mathbf{q}} \hbar\omega_{\zeta\mathbf{q}} \mathbf{M}_{\zeta\mathbf{q}} [\pm \underbrace{N_{\zeta\mathbf{q}} \mathbf{G}^{\lessgtr}(\epsilon \mp \hbar\omega_{\zeta\mathbf{q}})}_{\text{absorption contribution}} \mp \underbrace{(N_{\zeta\mathbf{q}} \overbrace{+1}^{\text{spontaneous}}) \mathbf{G}^{\lessgtr}(\epsilon \pm \hbar\omega_{\zeta\mathbf{q}})}_{\text{emission contribution}}] \mathbf{M}_{\zeta\mathbf{q}}, \tag{9}$$

and

$$\Xi^{r,a}_{\gamma}(\epsilon) = \pm\frac{1}{2}[\Xi^{>}_{\gamma}(\epsilon) - \Xi^{<}_{\gamma}(\epsilon)] + \frac{i}{2\pi}\mathcal{P}\int \mathrm{d}\epsilon' \frac{\Xi^{>}_{\gamma}(\epsilon') - \Xi^{<}_{\gamma}(\epsilon')}{\epsilon - \epsilon'}, \tag{10}$$

$N_{\zeta\mathbf{q}}$ is the occupation number of the radiation modes $\zeta\mathbf{q}$. These modes form the photon bath which is assumed to be in an equilibrium or quasi-equilibrium state of temperature T_γ and chemical potential μ_γ. The chemical potential can indeed be nonzero when the photon source cannot be modeled by a black body, like the radiation obtained from optical transitions in semiconducting matter [37]. The function $\Xi_\gamma(\epsilon)$ has the dimension of *energy*^{2}.

We separate the three essential contributions of the electron-photon interaction in equation (9): the two induced processes which include the absorption (*abs*) and the stimulated emission (*em*,*st*), and the spontaneous emission (*em*,*sp*) which is independent of the occupation number of the photon bath and is non-zero in the vacuum state [41]. The function Ξ_γ is split as

$$\Xi^{\lessgtr}_{\gamma} = \Xi^{\lessgtr}_{abs} + \Xi^{\lessgtr}_{em,st} + \Xi^{\lessgtr}_{em,sp}, \tag{11}$$

with

$$\Xi^{\lessgtr}_{abs}(\epsilon) = \pm\sum_{\zeta\mathbf{q}} \hbar\omega_{\zeta\mathbf{q}} \mathbf{M}_{\zeta\mathbf{q}} N_{\zeta\mathbf{q}} \mathbf{G}^{\lessgtr}(\epsilon \mp \hbar\omega_{\zeta\mathbf{q}}) \mathbf{M}_{\zeta\mathbf{q}}, \tag{12a}$$

$$\Xi^{\lessgtr}_{em,st}(\epsilon) = \mp\sum_{\zeta\mathbf{q}} \hbar\omega_{\zeta\mathbf{q}} \mathbf{M}_{\zeta\mathbf{q}} N_{\zeta\mathbf{q}} \mathbf{G}^{\lessgtr}(\epsilon \pm \hbar\omega_{\zeta\mathbf{q}}) \mathbf{M}_{\zeta\mathbf{q}}, \tag{12b}$$

$$\Xi^{\lessgtr}_{em,sp}(\epsilon) = \mp\sum_{\zeta\mathbf{q}} \hbar\omega_{\zeta\mathbf{q}} \mathbf{M}_{\zeta\mathbf{q}} \mathbf{G}^{\lessgtr}(\epsilon \pm \hbar\omega_{\zeta\mathbf{q}}) \mathbf{M}_{\zeta\mathbf{q}}. \tag{12c}$$

The photon energy current thus inherits the Ξ_γ splitting, and it can be cast according to different viewpoints

$$I^{E}_{\gamma} = I^{E}_{abs} + I^{E}_{em,st} + I^{E}_{em,sp} \tag{13}$$

$$= I^{E}_{\mathrm{ind}} + I^{E}_{em,sp} \tag{14}$$

$$= I^{E}_{abs} + I^{E}_{em}. \tag{15}$$

3.2. Energy conservation

In the case of the self-consistent Born approximation, the energy has to be conserved in the total system [44]

$$\langle \dot{H} \rangle = \langle \dot{H}_L + \dot{H}_R + \dot{H}_\gamma + \dot{H}_0 + \dot{H}_T + \dot{H}_{\mathrm{int}} \rangle = 0. \tag{16}$$

The two first terms are known from [12], $\dot{H}_{\alpha\in L,R} = -\frac{2}{h}\mathrm{Re}\,\mathrm{Tr}\int \mathrm{d}\epsilon\epsilon[\mathbf{G}^{r}\Sigma^{<}_{\alpha} + \mathbf{G}^{<}\Sigma^{a}_{\alpha}](\epsilon)$ with $\Sigma^{<,a}_{\alpha}$ the reservoir self-energies [42]. Energy currents related to the central region, to the transfer process and to light-matter interaction are zero for steady-state operating: $\langle \dot{H}_0 \rangle = 0, \langle \dot{H}_T \rangle = 0$, and $\langle \dot{H}_{\mathrm{int}} \rangle = 0$. We verified energy conservation starting from the photon energy current of equation (8) together with the expressions of $\langle \dot{H}_L \rangle$ and $\langle \dot{H}_R \rangle$ given in [12]. In order to eliminate the reservoir self-energies $\Sigma^{\lessgtr}_{L,R}$, we used the property $\mathrm{Tr}[\Sigma^{<}\mathbf{G}^{>} - \Sigma^{>}\mathbf{G}^{<}] = 0$ where $\Sigma^{\lessgtr} = \sum_{\alpha\in L,R,\mathrm{int}} \Sigma^{\lessgtr}_{\alpha}$ is the total self-energy [42]. Then, we evidenced the following quantity $\epsilon\Sigma^{\lessgtr}_{\gamma}(\epsilon) - \hbar\omega_{\zeta\mathbf{q}}\widetilde{\Sigma}^{\lessgtr}_{\gamma}(\epsilon)$, and performed the changes of integration variable $\epsilon' = \epsilon \pm \hbar\omega_{\zeta\mathbf{q}}$.

[3] Inside this derivation, the Hartree-like term is zero from the Wick's theorem using the model hamiltonian of equation (2).

3.3. Absorption and emission rates

Similarly, the photon current $I_\gamma(t) = -\langle \dot{N}_\gamma \rangle(t)$ can be derived relying on previous mixed Green's functions $\mathfrak{B}^t_{mn,\zeta\mathbf{q}}(t,t')$ defined equation (4). We get

$$I_\gamma(t) = \frac{1}{\hbar}\,\mathrm{Re}\,\mathrm{Tr}\int \mathrm{d}t_1[\mathbf{G}^r(t,t_1)\widetilde{\mathbf{\Sigma}}^<_\gamma(t_1,t) + \mathbf{G}^<(t,t_1)\widetilde{\mathbf{\Sigma}}^a_\gamma(t_1,t)], \tag{17}$$

with

$$\widetilde{\mathbf{\Sigma}}^\lessgtr_\gamma(t,t') = \sum_{\zeta\mathbf{q}} \mathbf{M}_{\zeta\mathbf{q}}(t)\mathbf{G}^\lessgtr(t,t')\widetilde{D}^{0\lessgtr}_{\zeta\mathbf{q}}(t,t')\mathbf{M}_{\zeta\mathbf{q}}(t'). \tag{18}$$

For steady-state operation, we obtained

$$I_\gamma = \frac{1}{\hbar}\,\mathrm{Re}\,\mathrm{Tr}\int \frac{\mathrm{d}\epsilon}{2\pi}[\mathbf{G}^r\widetilde{\mathbf{\Sigma}}^<_\gamma + \mathbf{G}^<\widetilde{\mathbf{\Sigma}}^a_\gamma](\epsilon), \tag{19}$$

where

$$\widetilde{\mathbf{\Sigma}}^\lessgtr_\gamma = \sum_{\zeta\mathbf{q}} \mathbf{M}_{\zeta\mathbf{q}}[\pm N_{\zeta\mathbf{q}}\mathbf{G}^\lessgtr(\epsilon \mp \hbar\omega_{\zeta\mathbf{q}}) \mp (N_{\zeta\mathbf{q}}+1)\mathbf{G}^\lessgtr(\epsilon \pm \hbar\omega_{\zeta\mathbf{q}})]\mathbf{M}_{\zeta\mathbf{q}}, \tag{20}$$

and still

$$\widetilde{\mathbf{\Sigma}}^{r,a}_\gamma(\epsilon) = \pm\frac{1}{2}[\widetilde{\mathbf{\Sigma}}^>_\gamma(\epsilon) - \widetilde{\mathbf{\Sigma}}^<_\gamma(\epsilon)] + \frac{i}{2\pi}\mathcal{P}\int \mathrm{d}\epsilon' \frac{\widetilde{\mathbf{\Sigma}}^>_\gamma(\epsilon') - \widetilde{\mathbf{\Sigma}}^<_\gamma(\epsilon')}{\epsilon - \epsilon'}. \tag{21}$$

It is worth comparing the function $\widetilde{\mathbf{\Sigma}}_\gamma$ with the interaction self-energy $\mathbf{\Sigma}_\gamma$ which appears in the Dyson equation for an electron interacting with light radiation [23, 43]

$$\mathbf{\Sigma}^\lessgtr_\gamma(\epsilon) = \sum_{\zeta\mathbf{q}} \mathbf{M}_{\zeta\mathbf{q}}[N_{\zeta\mathbf{q}}\mathbf{G}^\lessgtr(\epsilon \mp \hbar\omega_{\zeta\mathbf{q}}) + (N_{\zeta\mathbf{q}}+1)\mathbf{G}^\lessgtr(\epsilon \pm \hbar\omega_{\zeta\mathbf{q}})]\mathbf{M}_{\zeta\mathbf{q}}. \tag{22}$$

Sign changes between $\widetilde{\mathbf{\Sigma}}^<_\gamma$ and $\mathbf{\Sigma}^<_\gamma$ are intuitive: absorption(emission) means that a photon is flowing from the photon bath(central region) to the central region(photon bath). Without these sign changes, $\mathrm{Re}\,\mathrm{Tr}\int\frac{\mathrm{d}\epsilon}{2\pi}[\mathbf{G}^r\mathbf{\Sigma}^<_\gamma + \mathbf{G}^<\mathbf{\Sigma}^a_\gamma](\epsilon) = 0$ (to be compared with equation (19)), which fulfills the condition of current conservation along the nanodevice [42].

Similarly to the case of the photon energy current, it is meaningful to distinguish between the three radiative processes of the electron-photon interaction throughout

$$\widetilde{\mathbf{\Sigma}}^\lessgtr_\gamma = \underbrace{\widetilde{\mathbf{\Sigma}}^\lessgtr_{abs} + \widetilde{\mathbf{\Sigma}}^\lessgtr_{em,st}}_{\text{induced processes}} + \widetilde{\mathbf{\Sigma}}^\lessgtr_{em,sp}, \tag{23}$$

with

$$\widetilde{\mathbf{\Sigma}}^\lessgtr_{abs}(\epsilon) = \pm\sum_{\zeta\mathbf{q}} N_{\zeta\mathbf{q}}\mathbf{M}_{\zeta\mathbf{q}}\mathbf{G}^\lessgtr(\epsilon \mp \hbar\omega_{\zeta\mathbf{q}})\mathbf{M}_{\zeta\mathbf{q}}, \tag{24a}$$

$$\widetilde{\mathbf{\Sigma}}^\lessgtr_{em,st}(\epsilon) = \mp\sum_{\zeta\mathbf{q}} N_{\zeta\mathbf{q}}\mathbf{M}_{\zeta\mathbf{q}}\mathbf{G}^\lessgtr(\epsilon \pm \hbar\omega_{\zeta\mathbf{q}})\mathbf{M}_{\zeta\mathbf{q}}, \tag{24b}$$

$$\widetilde{\mathbf{\Sigma}}^\lessgtr_{em,sp}(\epsilon) = \mp\sum_{\zeta\mathbf{q}} \mathbf{M}_{\zeta\mathbf{q}}\mathbf{G}^\lessgtr(\epsilon \pm \hbar\omega_{\zeta\mathbf{q}})\mathbf{M}_{\zeta\mathbf{q}}. \tag{24c}$$

The derivation of I_γ equation (19) provides general expressions for the radiative rates in the stationary case. Indeed, we decompose $\langle \dot{N}_\gamma \rangle = -R_{abs} + R_{em,st} + R_{em,sp}$ and then identify (using the cycling property of the trace)

$$R_{abs} = \frac{1}{h}\sum_{\zeta\mathbf{q}} N_{\zeta\mathbf{q}}\int \mathrm{d}\epsilon\,\mathcal{T}^-(\epsilon,\hbar\omega_{\zeta\mathbf{q}}), \tag{25a}$$

$$R_{em,st} = \frac{1}{h}\sum_{\zeta\mathbf{q}} N_{\zeta\mathbf{q}}\int \mathrm{d}\epsilon\,\mathcal{T}^+(\epsilon,\hbar\omega_{\zeta\mathbf{q}}), \tag{25b}$$

$$R_{em,sp} = \frac{1}{h}\sum_{\zeta\mathbf{q}} \int \mathrm{d}\epsilon\,\mathcal{T}^+(\epsilon,\hbar\omega_{\zeta\mathbf{q}}), \tag{25c}$$

where

$$\mathcal{T}^\pm(\epsilon,\hbar\omega_{\zeta\mathbf{q}}) = \mathrm{Tr}[\mathbf{M}_{\zeta\mathbf{q}}\mathbf{G}^<(\epsilon \pm \hbar\omega_{\zeta\mathbf{q}})\mathbf{M}_{\zeta\mathbf{q}}\mathbf{G}^>(\epsilon)]. \tag{26}$$

Equations (25a–25c) reiterate the formula provided by Aeberhard in [45] from an analogy between the Boltzmann and Dyson equations.

3.4. Spectral photon currents

From the partition presented equation (23), it is possible to derive the three spectral photon currents using the photon density of states $\mathcal{D}_{\zeta\mathbf{u}}(\hbar\omega)$ in the large volume limit

$$r^{abs}_{\zeta\mathbf{u}}(\hbar\omega) = N_{\zeta\mathbf{u}}(\hbar\omega)\mathcal{D}_{\zeta\mathbf{u}}(\hbar\omega)\frac{1}{h}\int \mathrm{d}\epsilon\,\mathcal{T}^-_{\zeta\mathbf{u}}(\epsilon,\hbar\omega), \tag{27a}$$

$$r^{em,st}_{\zeta\mathbf{u}}(\hbar\omega) = -N_{\zeta\mathbf{u}}(\hbar\omega)\mathcal{D}_{\zeta\mathbf{u}}(\hbar\omega)\frac{1}{h}\int \mathrm{d}\epsilon\,\mathcal{T}^+_{\zeta\mathbf{u}}(\epsilon,\hbar\omega), \tag{27b}$$

$$r^{em,sp}_{\zeta\mathbf{u}}(\hbar\omega) = -\mathcal{D}_{\zeta\mathbf{u}}(\hbar\omega)\frac{1}{h}\int \mathrm{d}\epsilon\,\mathcal{T}^+_{\zeta\mathbf{u}}(\epsilon,\hbar\omega). \tag{27c}$$

We have introduced the direction of light propagation $\mathbf{u} = \mathbf{q}/||\mathbf{q}||$ and abbreviated the frequency by writing ω.

The radiation is treated as a third terminal here, in contrast with other developments where the photon Green's functions are fully taken into account with their own dynamics [46]. However, the present derivations allow us to provide radiation properties from the knowledge of the matter, in terms of electron Green's functions, via the trace of $\mathbf{M}_{\zeta\mathbf{u}}\mathbf{G}^<(\epsilon \pm \hbar\omega)\mathbf{M}_{\zeta\mathbf{u}}\mathbf{G}^>(\epsilon)$ (see equation (26)). This function depends on both the electron and photon energies, and it is connected to the polarization insertion of the interaction dynamics [47]. It is also interesting to introduce the induced spectral current $r^{\mathrm{ind}} = r^{abs} + r^{em,st}$ given by

$$r^{\mathrm{ind}}_{\zeta\mathbf{u}}(\hbar\omega) = N_{\zeta\mathbf{u}}(\hbar\omega)\mathcal{D}_{\zeta\mathbf{u}}(\hbar\omega)\mathcal{A}_{\zeta\mathbf{u}}(\hbar\omega), \tag{28}$$

where

$$\mathcal{A}_{\zeta\mathbf{u}}(\hbar\omega) = \frac{1}{h}\int \mathrm{d}\epsilon[\mathcal{T}^-_{\zeta\mathbf{u}} - \mathcal{T}^+_{\zeta\mathbf{u}}](\epsilon,\hbar\omega) \tag{29}$$

is a rate of net absorption (if $\mathcal{A} > 0$) or gain (if $\mathcal{A} < 0$) in the optoelectronic device. Taking advantage of the equality of $\int \mathrm{d}\epsilon \mathcal{T}^{-}_{\zeta\mathbf{u}}(\epsilon, \hbar\omega) = \int \mathrm{d}\epsilon \mathcal{T}^{-}_{\zeta\mathbf{u}}(\epsilon + \hbar\omega, \hbar\omega)$, the spectral current r^{ind} is shaped into

$$r^{\mathrm{ind}}_{\zeta\mathbf{u}}(\hbar\omega) = \frac{1}{h}\mathcal{D}_{\zeta\mathbf{u}}(\hbar\omega)N_{\zeta\mathbf{u}}(\hbar\omega)\int \mathrm{d}\epsilon \mathcal{T}^{+}_{\zeta\mathbf{u}}(\epsilon, \hbar\omega)\,\mathcal{B}^{-1}_{\zeta\mathbf{u}}(\epsilon, \hbar\omega), \tag{30}$$

with

$$\begin{aligned}\mathcal{B}_{\zeta\mathbf{u}}(\epsilon, \hbar\omega) &= \left[\frac{\mathrm{Tr}[\mathbf{M}_{\zeta\mathbf{u}}\mathbf{G}^{<}(\epsilon)\mathbf{M}_{\zeta\mathbf{u}}\mathbf{G}^{>}(\epsilon + \hbar\omega)]}{\mathrm{Tr}\,[\mathbf{M}_{\zeta\mathbf{u}}\mathbf{G}^{<}(\epsilon + \hbar\omega)\mathbf{M}_{\zeta\mathbf{u}}\mathbf{G}^{>}(\epsilon)]} - 1\right]^{-1} \\ &= \left[\frac{\mathcal{T}^{-}_{\zeta\mathbf{u}}(\epsilon + \hbar\omega, \hbar\omega)}{\mathcal{T}^{+}_{\zeta\mathbf{u}}(\epsilon, \hbar\omega)} - 1\right]^{-1}.\end{aligned} \tag{31}$$

Using the dimensionless function $\mathcal{B}_{\zeta\mathbf{u}}(\epsilon, \hbar\omega)$, we finally formulate the photon particle and energy currents as follows

$$\begin{aligned}I_{\gamma} = \frac{1}{h}\sum_{\zeta}\int \mathrm{d}\,\Omega_{\mathbf{u}}\int \mathrm{d}(\hbar\omega)\mathcal{D}_{\zeta\mathbf{u}}(\hbar\omega) \\ \times \int \mathrm{d}\epsilon \mathcal{T}^{+}_{\zeta\mathbf{u}}(\epsilon, \hbar\omega)[N_{\zeta\mathbf{u}}(\hbar\omega)\mathcal{B}^{-1}_{\zeta\mathbf{u}}(\epsilon, \hbar\omega) - 1],\end{aligned} \tag{32}$$

$$\begin{aligned}I^{E}_{\gamma} = \frac{1}{h}\sum_{\zeta}\int \mathrm{d}\,\Omega_{\mathbf{u}}\int \mathrm{d}(\hbar\omega)\mathcal{D}_{\zeta\mathbf{u}}(\hbar\omega)\hbar\omega \\ \times \int \mathrm{d}\epsilon \mathcal{T}^{+}_{\zeta\mathbf{u}}(\epsilon, \hbar\omega)[N_{\zeta\mathbf{u}}(\hbar\omega)\mathcal{B}^{-1}_{\zeta\mathbf{u}}(\epsilon, \hbar\omega) - 1],\end{aligned} \tag{33}$$

where $\mathrm{d}\,\Omega_{\mathbf{u}}$ is the elementary solid angle around the direction $\mathbf{u}$ along which the light propagates. It is interesting to point out the similar expressions we have for these currents: they are both written as the product of a two-dimensional spectral quantity $\mathcal{D}_{\zeta\mathbf{u}}(\hbar\omega)\mathcal{T}^{+}_{\zeta\mathbf{u}}(\epsilon, \hbar\omega)[N_{\zeta\mathbf{u}}(\hbar\omega)\mathcal{B}^{-1}_{\zeta\mathbf{u}}(\epsilon, \hbar\omega) - 1]$ multiplied by the photon energy $\hbar\omega$ at the power zero for the particle current, and at the power one for the energy current.

3.5. Quasi-equilibrium limits

Within NEGF formalism, the electron-photon interaction is described using the self-consistent Born approximation in terms of electron and photon Green's functions. The approach is original in the sense that it is in fact not necessary to define local thermodynamic parameters to obtain particle, energy or entropy currents which flow outside the out-of-equilibrium central region. In devices where the central region reaches the nanoscale, particles experience non-thermal states while the device is working. It is not a simple task to define local temperature, and electrochemical potential in the interacting central region [48, 49]. Indeed, all the particle statistics is encoded in NEGF formalism [50]. However, if NEGFs can be represented by quasi-equilibrium Green's functions, they will verify a Kubo-Martin-Schwinger relation [51] $\mathbf{G}^{>}(\epsilon) = \mathbf{G}^{<}(\epsilon)\mathrm{e}^{\frac{\epsilon-\mu}{k_{\mathrm{B}}T}}$, where μ and T represent the electronic chemical potential and temperature respectively. This relation generalizes the following properties of the Fermi–Dirac and Bose–Einstein functions: $1 - f(\epsilon) = \mathrm{e}^{\frac{\epsilon-\mu}{k_{\mathrm{B}}T}}f(\epsilon)$ and $N(\hbar\omega) + 1 = \mathrm{e}^{\frac{\hbar\omega}{k_{\mathrm{B}}T}}N(\hbar\omega)$.

More generally, let us consider the case of a semiconductor in which electrons inside the conduction band, and holes inside the valence band experience separate quasi-equilibrium states characterized by two different chemical potentials and temperatures, $\mu_{c,v}$ and $T_{c,v}$. In that case, the diagonal components of Green's functions follow local Kubo–Martin–Schwinger relations

$$[\mathbf{G}^{>}]_{n}(\epsilon) = [\mathbf{G}^{<}]_{n}(\epsilon)\mathrm{e}^{\frac{\epsilon-\mu_{n}}{k_{\mathrm{B}}T_{n}}}, \tag{34}$$

where $(n \in c, v)$ refers to the band index. Thanks to these relations, simplifications occur in the expression of $\mathcal{B}$, equation (31). In particular for $T = T_c = T_v$, $\mathcal{B}$ no longer depends on the electron energy ϵ, and it follows

$$\mathcal{B}(\hbar\omega) = \left[\exp\left(\frac{\hbar\omega - (\mu_c - \mu_v)}{k_{\mathrm{B}}T}\right) - 1\right]^{-1}, \tag{35}$$

in which one can define $T_E = T$ and $\mu_E = (\mu_c - \mu_v)$, the temperature and chemical potential of the spontaneously emitted radiation [52]. Hence we obtain the full Bose–Einstein statistic function that happens in the so-called generalized Planck's law for the emission [52, 53], that was also discussed in photovoltaic cells of quantum dot arrays using NEGFs [54], and notably used to determine the thermopower from optical measurements [55].

In the quasi-equilibrium limit, $\mathcal{B}$ does not depend on ϵ, which allows us to write the spectral emission current as

$$r^{em,sp}_{\zeta\mathbf{u}}(\hbar\omega) = -\mathcal{B}(\hbar\omega)\mathcal{D}_{\zeta\mathbf{u}}(\hbar\omega)\mathcal{A}_{\zeta\mathbf{u}}(\hbar\omega). \tag{36}$$

Using equations (28) and (29), the two quasi-equilibrium limits of the photon particle and energy currents finally read as

$$\begin{aligned}I_{\gamma} = \sum_{\zeta}\int \mathrm{d}\,\Omega_{\mathbf{u}}\int \mathrm{d}(\hbar\omega)\mathcal{D}_{\zeta\mathbf{u}}(\hbar\omega) \\ \times [N(\hbar\omega) - \mathcal{B}(\hbar\omega)]\mathcal{A}_{\zeta\mathbf{u}}(\hbar\omega),\end{aligned} \tag{37}$$

$$\begin{aligned}I^{E}_{\gamma} = \sum_{\zeta}\int \mathrm{d}\,\Omega_{\mathbf{u}}\int \mathrm{d}(\hbar\omega)\hbar\omega\mathcal{D}_{\zeta\mathbf{u}}(\hbar\omega) \\ \times [N(\hbar\omega) - \mathcal{B}(\hbar\omega)]\mathcal{A}_{\zeta\mathbf{u}}(\hbar\omega).\end{aligned} \tag{38}$$

Equations (37) and (38) are similar to the ones obtained in [46] dealing with non-equilibrium photon Green's functions. Interestingly, our approach suggests that a generalized energy flow law would involve two-dimensional spectral functions

$$j^{E}_{\zeta\mathbf{u}}(\epsilon, \hbar\omega) = a_{\zeta\mathbf{u}}(\epsilon, \hbar\omega)[N_{\zeta\mathbf{u}}(\hbar\omega) - \mathcal{B}_{\zeta\mathbf{u}}(\epsilon, \hbar\omega)] \tag{39}$$

with

$$a_{\zeta\mathbf{u}}(\epsilon, \hbar\omega) = [\mathcal{T}^{-}_{\zeta\mathbf{u}}(\epsilon + \hbar\omega, \hbar\omega) - \mathcal{T}^{+}_{\zeta\mathbf{u}}(\epsilon, \hbar\omega)]/h, \tag{40}$$

in the case of a non-equilibrium nanosystem, for which charge and energy currents are given by equations (32) and (33).

Table 1. Efficiency notations and definitions which will be used for a photovoltaic (*PV*), cooling by heating (*CBH*) and a joint cooling and electrical energy production (*JCEP*) nanodevices. For *PV* and *JCEP* devices, $I_L^e V \leqslant 0$. For a *CBH* device, $I_R^h \geqslant 0$, and for a *JCEP* device, $I_L^h \geqslant 0$. In all cases, $I_{abs}^h \geqslant 0$.

Nanodevice (*ND*)	η_{ND}
PV	$\eta_{PV} = -\frac{I_L^e V}{I_{abs}^h}$
$(T_L = T_R, \mu_L > \mu_R)$	
CBH	$\eta_{CBH} = \frac{I_R^h}{I_{abs}^h}$
$(T_L > T_R, \mu_L = \mu_R)$	
JCEP	$\eta_{JCEP} = \frac{I_L^h - I_L^e V}{I_{abs}^h}$
$(T_L < T_R, \mu_L > \mu_R)$	$= \eta_{CBH} + \eta_{PV}$
Standard engine	η^{rev}
Carnot machine (C)	$\eta_{\text{C}}^{ch} = 1 - \frac{T_c}{T_h}$
$(T_{c(\text{cold})} < T_{h(\text{hot})})$	
Refrigeration (⊛)	$\eta_{\circledast}^{ch} = \frac{T_c}{T_h - T_c}$
Heat pump (≀≀≀)	$\eta_{\wr\wr\wr}^{ch} = \frac{T_h}{T_h - T_c}$
Trithermal heat engine (3*T*)	
$(T_c < T_{i(\text{intermediate})} < T_h)$	$\eta_{3T}^{cih} = \eta_{\text{C}}^{ih} \times \eta_{\circledast}^{ci}$

4. Entropy current

The entropy current I^S flowing from the central region to the reservoirs is calculated in terms of electron Green's function and self-energies using the expression of photon energy current given equation (8).

4.1. Spectral entropy current

The device is an open interacting nanosystem connected to three reservoirs: the two electron left and right reservoirs, and the photon bath. In this three-terminal configuration, the entropy current flowing from the central region to the three reservoirs is defined as

$$I^S = \frac{I_L^h}{T_L} + \frac{I_R^h}{T_R} + \frac{I_\gamma^h}{T_\gamma} \tag{41}$$

$$= -\frac{\langle \dot{H}_L \rangle - \mu_L \langle \dot{N}_L \rangle}{T_L} - \frac{\langle \dot{H}_R \rangle - \mu_R \langle \dot{N}_R \rangle}{T_R} - \frac{\langle \dot{H}_\gamma - \mu_\gamma \dot{N}_\gamma \rangle}{T_\gamma} \tag{42}$$

$$= \frac{I_L^E}{T_L} + \frac{I_R^E}{T_R} - I_L \left[\frac{\mu_L}{T_L} + \frac{\mu_R}{T_R} \right] + \frac{I_\gamma^E}{T_\gamma} - I_\gamma \frac{\mu_\gamma}{T_\gamma}, \tag{43}$$

in which we use the relation $\langle \dot{N}_L \rangle = -\langle \dot{N}_R \rangle$ guaranteed by charge conservation.

Implementing results of sections 3.1 and 3.2 in equation (41), we are hence able to derive the entropy current in terms of Green's functions from the spectral entropy current $J^S(\epsilon)$ as follows

$$I^S = \int \mathrm{d}\epsilon J^S(\epsilon), \tag{44}$$

with

$$J^S(\epsilon) = \frac{2}{h} \mathrm{Re}\,\mathrm{Tr}[\mathbf{G}^r \mathfrak{S}^< + \mathbf{G}^< \mathfrak{S}^a](\epsilon), \tag{45}$$

and

$$\mathfrak{S}^{<,a}(\epsilon) = \sum_{\alpha \in L,R} \frac{(\epsilon - \mu_\alpha) \mathbf{\Sigma}_\alpha^{<,a}(\epsilon)}{T_\alpha} + \frac{1}{2} \frac{\mathbf{\Xi}_\gamma^{<,a}(\epsilon) - \mu_\gamma \widetilde{\mathbf{\Sigma}}_\gamma^{<,a}(\epsilon)}{T_\gamma}. \tag{46}$$

The entropy current flowing from the central region to the reservoirs is equal to the rate of entropy production $\Pi = I^S$ for nanosystems maintained in out-of-equilibrium steady states [56].

4.2. Entropy production is recast in terms of efficiencies

For photovoltaic-thermoelectric converters, we define the nanodevice efficiency as the ratio of the output electrical power or useful heat current to the input power in the form of light, which is given by the heat current of the absorbed photons, I_{abs}^h. This definition contrasts with 'the maximal power conversion efficiency' defined in practice at maximal output power, and where the denominator is the incident radiant power; it thus does not depend on the processes undergone by the system [57].

In this section, we focus on three devices based on a central region interacting with light: a photovoltaics (*PV*), a refrigerator based on a cooling by heating process (*CBH*) [32], and finally a joint device which provides both cooling and electrical energy production (*JCEP*) [35]. For the three nanodevices, the rate of entropy production is recast in terms of efficiencies according to the device, as Whitney proposed in [58]. Indeed, all nanodevices (*ND*) provide the same formal rate of entropy production

$$\Pi = \Pi_0 [\eta_{ND}^{\text{rev}} - \eta_{ND}], \tag{47}$$

where η_{ND}^{rev} is the efficiency of the reversible nanodevice, $\eta_{ND}^{\text{rev}} I_{abs}^h$ is the output power in the reversible nanodevice, and $\Pi_0 \eta_{ND}^{\text{rev}}$ is the maximum rate of entropy production achievable in the nanodevice. Ratio Π_0/Π reflects how close to the maximum efficiency the device is working.

Table 1 summarizes the definitions and notations of the relevant efficiencies discussed for the three nanodevices. These efficiencies are named thermodynamic efficiencies as they can be manipulated following the laws of thermodynamics.

4.2.1. Standard photovoltaics. For $T_L = T_R$, we can derive the photovoltaic case

$$\Pi = \frac{I_{abs}^h}{T_L} \left[\underbrace{\left(1 - \left| \frac{I_{em}^h}{I_{abs}^h} \right| \right) \eta_{\text{C}}^{LS}}_{\eta_{PV}^{\text{rev}}} - \eta_{PV} \right], \tag{48}$$

where $I^h_{em} = I^h_{em,st} + I^h_{em,sp}$, and $I^h_{em,st(p)} = I^E_{em,st(p)} + \mu_\gamma R_{em,st(p)}$. We always have $I^h_{em} < 0$ while $I^h_{abs} > 0$. The Carnot efficiency η^{LS}_C is defined in table 1.

Here, it can be worth deriving the related electroluminescent (*EL*) case, for which $N_\gamma = 0$ implies $I^h_{\text{ind}} = 0$,

$$\Pi = I^e_L V \frac{T_E - T_L}{T_E T_L}[\eta^{LE}_{\text{\Large\wasylozenge}} - \eta_{EL}], \tag{49}$$

where $\eta_{EL} = -\frac{I^h_{em,sp}}{P^e}$ (with $P^e = I^e_L V \geqslant 0$) is the efficiency of the electroluminescent device, and T_E replaces T_γ is the temperature of the photon bath formed by electroluminescence.

The efficiency of the reversible photovoltaic nanodevice is reduced compared to the Carnot limit: from equation (48), the maximum value of efficiency is $\eta^{\text{rev}}_{PV} = \eta^{LS}_C\left[1 - |\frac{I^h_{em}}{I^h_{abs}}|\right]$. This maximal efficiency may be compared to the Landsberg's limit [59, 60]: $\eta_{\text{Landsberg}} = \eta^{AS}_C\left[1 - \frac{1}{3}\frac{T_A}{T_\gamma}\left(1 + \frac{T_A}{T_\gamma} + \frac{T^2_A}{T^2_\gamma}\right)\right]$, where A stands for ambient, and it corresponds to T_L in this work. Landsberg reconsidered the limit of the Carnot efficiency as the upper limit for photovoltaics. Starting from the model of dithermal engine, he included the energy and entropy fluxes related to the emission process. In the Landsberg's approach, the central region is a converter in a state of equilibrium, and it behaves as a black body emitting photons at temperature T_C (C stands for converter). Landsberg demonstrated that the maximal efficiency of the reversible device, $\eta_{\text{Landsberg}}$, is reached when $T_C = T_A$. The Landsberg's approach ignores the details of electron properties in the converter, which is also assumed at equilibrium. However, despite these differences, the NEGF-based expression of entropy production rate, equation (48), provides similar conclusions to those of Landsberg: the maximum efficiency is always lesser than the Carnot limit of a heat engine producing work from electron and photon reservoirs.

4.2.2. Cooling by heating process. We discuss the coefficient of performance of a cooling by heating process as proposed in [32] with $T_L > T_R$ and $V = 0$ (see table 1 for the efficiency definitions),

$$\Pi = \frac{I^h_{abs}}{T_L}\left[\underbrace{\left(1 - \left|\frac{I^h_{em}}{I^h_{abs}}\right|\right)\eta^{RLS}_{3T}}_{\eta^{\text{rev}}_{CBH}} - \eta_{CBH}\right]. \tag{50}$$

From this formula, we deduce for this original cooling process

$$\eta_{CBH} = \frac{T_R}{T_L - T_R}\left[\left(1 - \left|\frac{I^h_{em}}{I^h_{abs}}\right|\right)\eta^{LS}_C - \frac{T_L \Pi}{I^h_{abs}}\right], \tag{51}$$

which ressembles equation (11) of [32] with the additional reducing contribution $|\frac{I^h_{em}}{I^h_{abs}}|\eta^{LE}_C$ to the *CBH* coefficient of performance. Indeed, the emission processes were not included in the approach of [61], which was developed in the strong optical coupling regime. Moreover, in the recent model proposed by Wang and co-authors in [34] to verify the third law of thermodynamics, the cooling regime includes a parasitic emission in the regime of weak coupling to electron reservoirs, which involves a single emission wavelength.

4.2.3. Joint cooling and energy production. For a more general case, but with a specific device objective, we examine the joint cooling and energy production proposed in [35]. The joint process can be seen as a photovoltaic configuration with $T_L < T_R$, or a cooling by heating configuration with $V > 0$. It follows two expressions for the rate of entropy production

$$\Pi = I^h_{abs}\frac{T_R - T_L}{T_L T_R}[\eta^{\text{rev}}_{CBH} - \eta_{PV}(\eta^{RL}_{\circledast} - 1) - \eta_{JCEP}], \tag{52}$$

and

$$\Pi = \frac{I^h_{abs}}{T_R}\left[\eta^{\text{rev}}_{PV} - \eta_{CBH}\left(\frac{1 - \eta^{RL}_{\circledast}}{\eta^{RL}_{\circledast}}\right) - \eta_{JCEP}\right]. \tag{53}$$

From equations (52) and (53), we deduce

$$\eta^{RL}_{\circledast} < 1 \Rightarrow \eta^{\text{rev}}_{CBH} < \eta^{\text{rev}}_{JCEP} < \eta^{\text{rev}}_{PV}, \tag{54}$$

$$\eta^{RL}_{\circledast} > 1 \Rightarrow \eta^{\text{rev}}_{PV} < \eta^{\text{rev}}_{JCEP} < \eta^{\text{rev}}_{CBH}. \tag{55}$$

In terms of applications, it means that for $\eta^{RL}_{\circledast} < 1$, a joint process more efficiently converts the photon bath power than the *CBH* one as shown by Entin-Wohlman and co-authors in [35], and we outline here that for $\eta^{RL}_{\circledast} > 1$, a joint process also more efficiently converts the photon bath power than the *photovoltaic device*. Additionally, writing $\eta^{\text{rev}}_{JCEP} = \eta^{*}_{CBH} + \eta^{*}_{PV}$, equations (54) and (55) also show $\eta^{*}_{CBH} < \eta^{\text{rev}}_{CBH}$ and $\eta^{*}_{PV} < \eta^{\text{rev}}_{PV}$, which means that the single conversion (*CBH* or *PV*) in the hybrid device is always less efficient than in the corresponding standard device.

5. Discussing the entropy production in a two-level system including light-matter interaction

In this section, we discuss how the second law of thermodynamics is not automatically verified depending on the model used to simulate how the nanodevice works. We focus on a minimal model of QD-based nanojunction. Such ultimate nanostructures allow us to grasp the essentials of the energy conversion at the nanoscale level using three-terminal configurations [62–65]. These kinds of configurations provide the separation between the charge and heat transport, and, at the same time, motivate innovative experimental realizations, as demonstrated recently in [66] and [67].

5.1. Basics of the modeling

We model a photovoltaic-thermoelectric junction based on quantum dots as shown figure 1. We follow a simplified methodology within the framework of NEGFs. The central region is made of a quantum dot of 1 nm^3. The dot is described by two

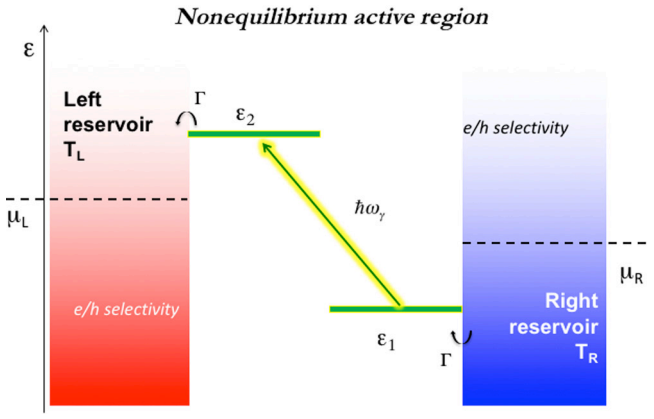

Figure 1. Level diagram of the junction: two discrete energy levels are available in the QD at energies $\varepsilon_1 = 0.5\,\mathrm{eV}$ and $\varepsilon_2 = -0.5\,\mathrm{eV}$ respectively. Level 1(2) is connected to the right(left) electron reservoir only, which provides a perfect electron/hole selectivity. For the numerical calculations, we use $\Gamma = 5\,10^{-2}\,\mathrm{eV}$ (half of the imaginary part of the advanced contact self-energy) and $M = 10^{-3}\,\mathrm{eV}$ (optical coupling). At the optical resonance, $\hbar\omega_\gamma = 1\,\mathrm{eV}$.

energy levels which interact with a resonant monochromatic radiation $\hbar\omega_\gamma$ through the optical coupling M_γ. The upper dot level ϵ_2 is only connected to the left electron reservoir while the lower level ϵ_1 is connected to the right one, which forces the charge separation without applying an electric field. The contact self-energies are given by $\Sigma^{r,a}_{L,R}(\epsilon) = \Lambda_{L,R}(\epsilon) \mp \mathrm{i}\Gamma_{L,R}(\epsilon)/2$ [68].

The rate of entropy production is calculated in the regime of strong coupling to reservoirs: the calculations are performed at the second order perturbation upon the optical coupling [69, 70]. This approach is valid as long as the optical coupling is lower than the transfer parameter, $M_\gamma \ll \Gamma_{L,R}$. The bias voltage is symmetrically applied $\mu_{L,R} = \pm\mathrm{eV}/2$ between the two electron reservoirs.

We specify the basic case of a linearly polarized monochromatic plane wave as an incident radiation of energy $\hbar\omega_\gamma$ and polarization ζ. Functions Ξ and $\widetilde{\Sigma}$ distinguish between the three radiative processes that are absorption, stimulated emission and spontaneous emission. For the monochromatic case, we used

$$\widetilde{\mathbf{\Sigma}}^{\lessgtr}_{abs}(\epsilon) = \pm N_\gamma \mathbf{M}_\gamma \mathbf{G}^{\lessgtr}(\epsilon \mp \hbar\omega_\gamma)\mathbf{M}_\gamma, \tag{56a}$$

$$\widetilde{\mathbf{\Sigma}}^{\lessgtr}_{em,st}(\epsilon) = \mp N_\gamma \mathbf{M}_\gamma \mathbf{G}^{\lessgtr}(\epsilon \pm \hbar\omega_\gamma)\mathbf{M}_\gamma, \tag{56b}$$

$$\widetilde{\mathbf{\Sigma}}^{\lessgtr}_{em,sp}(\epsilon) = \mp \mathbf{M}_\gamma \mathbf{G}^{\lessgtr}(\epsilon \pm \hbar\omega_\gamma)\mathbf{M}_\gamma, \tag{56c}$$

with $\mathbf{\Xi}^{\lessgtr}_{abs\text{ or }em,st} = \hbar\omega_\gamma \widetilde{\mathbf{\Sigma}}^{\lessgtr}_{abs\text{ or }em,st}$, and the real parts of the retarded and advanced components of the interaction self-energies are ignored. Optical coupling $\mathbf{M}_\gamma$ reads as $M_{nm,\omega_\gamma\zeta} = \sqrt{\hbar e^2/2V\epsilon_0\epsilon_r\omega_\gamma}\,P_{nm,\zeta}$ where $P_{nm,\zeta}$ is the momentum matrix element and V the volume of the interacting region.

For the two-level system, the problem is block-diagonal, and we use analytics to derive the spectral currents to the second order in $M_\gamma = M_{12,\omega_\gamma\zeta}$ in order to discuss the entropy production in the device.

5.2. Particle current

We focus on the spectral particle current $J_R(\epsilon)$, $I_R = \int \mathrm{d}\epsilon J_R(\epsilon)$, which is positive when an electrical power is produced. To the second order in M_γ, we find

$$J_R(\epsilon) = \frac{1}{h} M_\gamma^2 \mathcal{A}_1(\epsilon)\mathcal{A}_2(\epsilon + \hbar\omega_\gamma) \times [N_\gamma F^+_{RL}(\epsilon) - (N_\gamma + 1)F^-_{LR}(\epsilon + \hbar\omega_\gamma)], \tag{57}$$

with

$$\mathcal{A}_1(\epsilon) = \frac{\Gamma_R(\epsilon)}{(\epsilon - \Lambda_R(\epsilon) - \epsilon_1)^2 + \Gamma_R^2(\epsilon)/4} = -2\mathrm{Im}G^r_{11}(\epsilon), \tag{58}$$

$$\mathcal{A}_2(\epsilon) = \frac{\Gamma_L(\epsilon)}{(\epsilon - \Lambda_L(\epsilon) - \epsilon_2)^2 + \Gamma_L^2(\epsilon)/4} = -2\mathrm{Im}G^r_{22}(\epsilon), \tag{59}$$

and

$$F^\pm_{\alpha\beta}(\epsilon) = f_\alpha(\epsilon)[1 - f_\beta(\epsilon \pm \hbar\omega_\gamma)], \tag{60}$$

for $\alpha \in \{L, R\}$ and $\beta \in \{L, R\}$. Functions $F^\pm_{\alpha\beta}(\epsilon)$ naturally relate the photocurrent to the recent interpretation of the different contributions to the non-symmetrized noise in a quantum dot [71]. From $1 - f(\epsilon) = \mathrm{e}^{\frac{\epsilon-\mu}{k_\mathrm{B}T}} f(\epsilon)$ and $N(\hbar\omega) + 1 = \mathrm{e}^{\frac{\hbar\omega}{k_\mathrm{B}T}} N(\hbar\omega)$, $J_R(\epsilon)$ takes the form

$$J_R(\epsilon) = J_{abs}(\epsilon)[1 - \mathrm{e}^{-X(\epsilon)}], \tag{61}$$

with

$$X(\epsilon) = \frac{\epsilon + \hbar\omega_\gamma - \mu_L}{k_\mathrm{B}T_L} - \frac{\epsilon - \mu_R}{k_\mathrm{B}T_R} - \frac{\hbar\omega_\gamma}{k_\mathrm{B}T_\gamma}, \tag{62}$$

and

$$J_{abs}(\epsilon) = \frac{1}{h} M_\gamma^2 \mathcal{A}_1(\epsilon)\mathcal{A}_2(\epsilon + \hbar\omega_\gamma) \times N_\gamma f_R(\epsilon)(1 - f_L(\epsilon + \hbar\omega_\gamma)). \tag{63}$$

For $T_L = T_R$, the ϵ dependence of X drops out and $X = (\hbar\omega_\gamma\eta_\mathrm{C}^{L\gamma} - \mathrm{eV})/k_\mathrm{B}T_L$, where the Carnot efficiency η_C^{ch} is defined table 1. For reservoirs at the same temperature, the spectral particle current, and hence the charge current, vanishes at a voltage called open-circuit voltage in photovoltaics, $\mathrm{eV_{oc}} = \hbar\omega_\gamma\eta_\mathrm{C}^{L\gamma}$ given by $X = 0$. This result shows an interesting analogy with the observations made by Sánchez and Büttiker in [63]. Indeed, in the three-terminal configuration they propose, the heat current is controlled from Coulomb interaction instead of the light-matter one. The authors also evidence a stall voltage, equation (16) of [63], that is an analogue of V_oc, for which both charge and heat currents vanish. Comparing the two three-terminal configurations, this voltage is a fraction, equal to the Carnot efficiency, of the relevant energy quantum: the charging energy E_C in [63] versus the photon energy $\hbar\omega_\gamma$ in the configuration studied here. Moreover, the heat energy current in the right reservoir is also zero at this voltage in the current configuration due to $J^h_R(\epsilon) = (\epsilon - \mu_R)J_R(\epsilon)$. We moreover conclude that the heat current exchanged with the

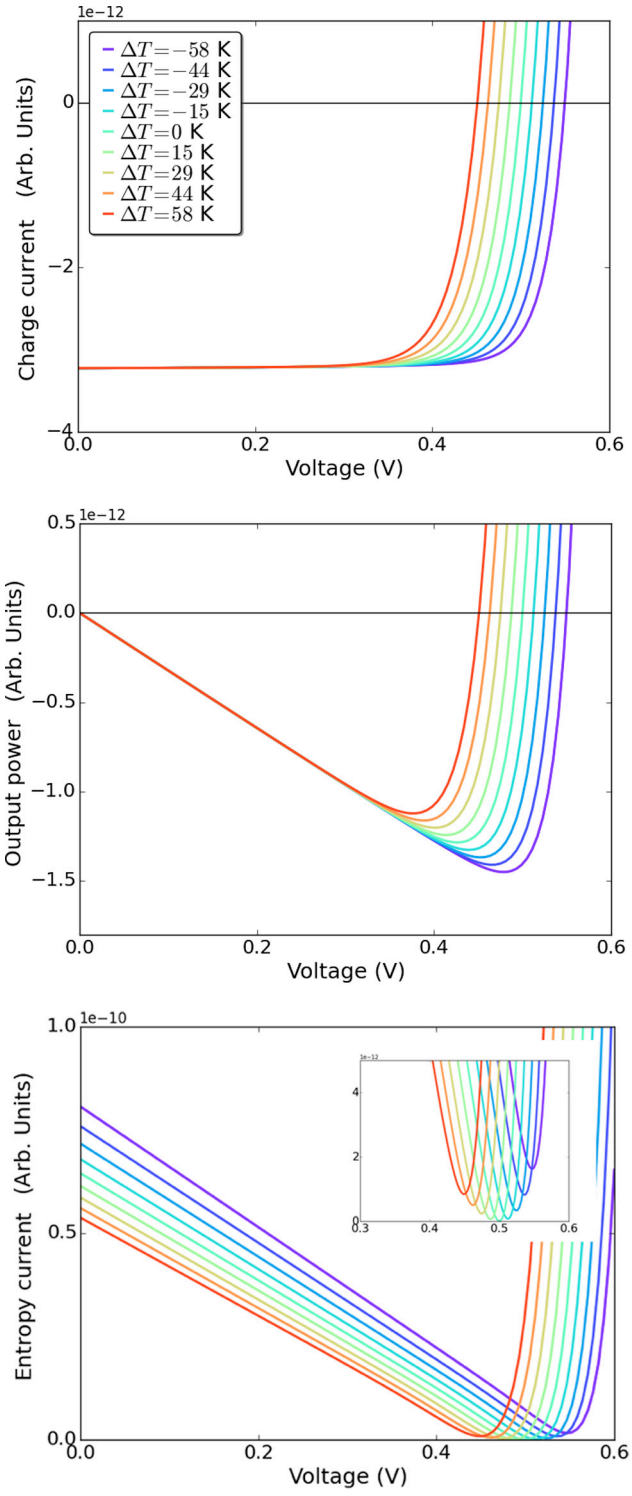

Figure 2. Charge current, output power and entropy current as a function of the voltage in the QD-based nanojunction for different temperature gradients $\Delta T = T_R - T_L$, $k_B T_L = 0.025$ eV and $k_B T_\gamma = 0.05$ eV.

photon reservoir is also zero at V_{oc} using this model, following $I^h_\gamma = \hbar\omega_\gamma I_\gamma = \hbar\omega_\gamma I_R$.

5.3. Entropy production

In this nanojunction architecture, the electron current cancels in the absence of light-matter interaction: the ballistic current is null. We have analytically verified that $\langle \dot{N}_L \rangle = -\langle \dot{N}_R \rangle = -\langle \dot{N}_\gamma \rangle$, which means that a carrier is added to(removed from) the left reservoir when a photon is removed/absorbed from (added/emitted to) the photon reservoir.

Assuming $T_L > T_R$, the spectral current $J^\Pi(\epsilon)$ is calculated using the relation $\langle \dot{N}_L \rangle = -\langle \dot{N}_R \rangle = -\langle \dot{N}_\gamma \rangle$:

$$\begin{aligned} J^\Pi(\epsilon) &= \epsilon J_R(\epsilon)\left[\frac{1}{T_L} - \frac{1}{T_R}\right] - J_R(\epsilon)\left[\frac{\mu_L}{T_L} - \frac{\mu_R}{T_R}\right] \\ &\quad + \hbar\omega_\gamma J_R(\epsilon)\left[\frac{1}{T_L} - \frac{1}{T_\gamma}\right] \\ &= J_R(\epsilon)\left[\frac{\epsilon + \hbar\omega_\gamma - \mu_L}{T_L} - \frac{\epsilon - \mu_R}{T_R} - \frac{\hbar\omega_\gamma}{T_\gamma}\right]. \end{aligned} \tag{64}$$

This spectral entropy current is not the one directly obtained from equations (45) and (46), but the integration of J^Π gives the rate of entropy production Π defined in equation (44). We can determine the sign of the entropy production from this integrand. Using equation (61) to express J_R, we obtain

$$J^\Pi(\epsilon) = k_B J_{abs}(\epsilon) X(\epsilon)[1 - e^{-X(\epsilon)}]. \tag{65}$$

In equation (65): on the one hand J_{abs} is always positive as it gives the rate of absorbed photons flowing to the active region, on the other hand the function $X[1 - e^{-X}]$ is always positive. The rate of entropy production is hence always positive, as it results from the direct integration of $J^\Pi(\epsilon)$. When $T_L = T_R$, the entropy current vanishes for $X = 0$ like the particle and heat currents, which was discussed in the previous section. Moreover, the analytical model also provides that the entropy production rate is concave at the open-circuit voltage since we obtain $\partial_V^2 I^\Pi(V_{oc}) = 2I_{abs}[\partial_V X(V_{oc})]^2 \geqslant 0$. The rate of the entropy production is minimum at open circuit conditions.

We numerically calculated the charge and entropy currents for various temperature gradients between the two electron reservoirs, in the optoelectronic junction depicted figure 1. The contact self-energies are given by a unique parameter Γ in the wide band limit $\mathrm{Im}\Sigma_{L,R} = -i\Gamma/2$ ($\Lambda = 0$) [68], and the other parameters are given figure 1. Characteristics of figure 2 show that cooling the right reservoir (cathode) in this configuration enhances the open-circuit voltage V_{oc} and the maximal output power. Additionally, the numerical results confirm that the rate of entropy production is always positive for all temperature differences and vanishes at V_{oc} for $T_L = T_R$, for which X does not depend on ϵ. Moreover, the numerical results show that the rate is minimum at V_{oc} and that the rate curve is concave around this point.

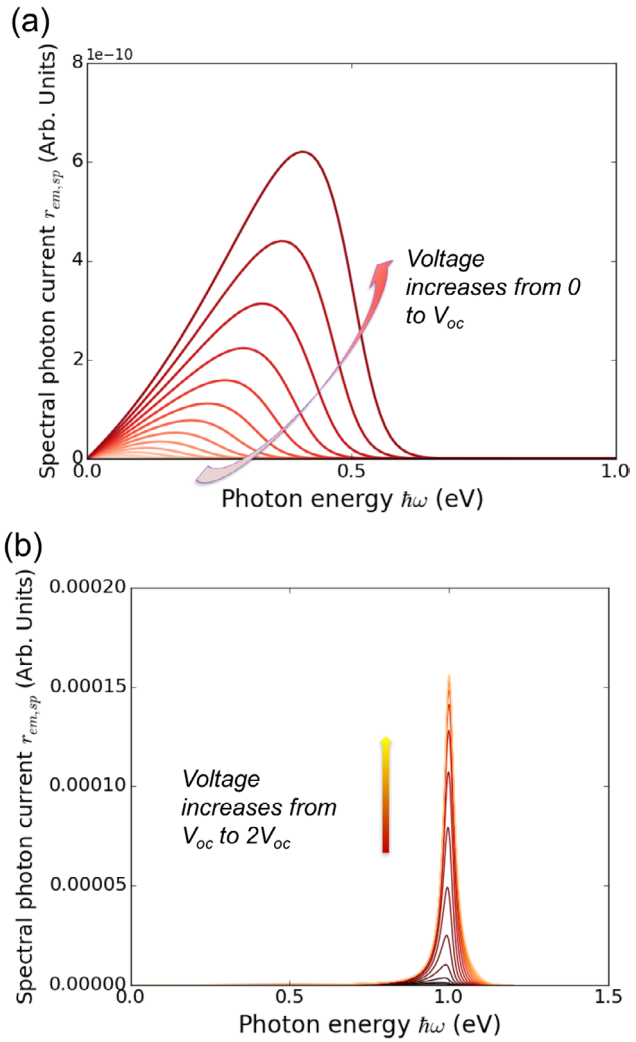

Figure 3. Spectral emission current in the QD-based nanojunction following equation (27*c*) for equal temperatures of electron reservoirs, varying the voltage (a) from zero to $V_{\rm oc} \approx 0.5$ V, and (b) from $V_{\rm oc}$ to $2V_{\rm oc}$.

5.4. Limits of traditional models

NEGF-based models for photovoltaics usually modify the interaction self-energies of equation (22) to determine the device functioning. Two post-treatments are done after the straightforward steps of derivation presented in sections 2 and 3. The Bose–Einstein function $N_{\zeta\mathbf{q}}$ is replaced by the number of incident photons estimated from the incoming photon flux [37], and the interaction self-energy term related to spontaneous emission is integrated over all possible photon states [72].

5.4.1. Photon number. Instead of the Bose–Einstein function, realistic modelings of solar cells introduce

$$N_\phi = \frac{I_\phi V}{\hbar\omega_\gamma C_0/\kappa}. \tag{66}$$

The number N_ϕ is calculated from the photon flux intensity at the surface of the earth $I_\phi \approx 10^3\,\mathrm{W m^{-2}}$, which accounts for the solid angle between the sun and the earth, the volume and the refractive index, V and κ, of the absorber (here the nanoscopic dot) and the speed of light in vacuum C_0.

5.4.2. Integrated spontaneous emission. In contrast with the two induced radiative processes, the self-energy term related to spontaneous emission does not explicitly depend on the properties of the incident radiation. For nanosystems strongly hybridized with electron reservoirs, the density of states broadens. It provides broad emission spectra for the set of parameters given figure 1, as illustrated figures 3(a) and (b) in the two ranges of voltage values below the open-circuit voltage and close to the QD gap, respectively. A transition occurs from black body radiation (figure 3(a)) to the luminescence peak typical of semiconductor emitters (figure 3(b)) [52]. It thus seems essential to integrate over all the possible transition energies of the interacting region [72]. We introduce the photon density of states $\rho(\hbar\omega) = V(\hbar\omega)^2\kappa/\pi^2\hbar^3C_0^3$ to reformulate

$$\widetilde{\Sigma}^{\lessgtr}_{em,sp}(\epsilon) = \mp\int \mathrm{d}(\hbar\omega)\rho(\hbar\omega) \times \mathbf{M}(\hbar\omega)\mathbf{G}^{\lessgtr}(\epsilon \pm \hbar\omega)\mathbf{M}(\hbar\omega), \tag{67a}$$

$$\Xi^{\lessgtr}_{em,sp}(\epsilon) = \mp\int \mathrm{d}(\hbar\omega)\rho(\hbar\omega)\hbar\omega \times \mathbf{M}(\hbar\omega)\mathbf{G}^{\lessgtr}(\epsilon \pm \hbar\omega)\mathbf{M}(\hbar\omega), \tag{67b}$$

where we assumed a polarization isotropy for the interacting nanosystem.

The two post-treatments can also be done in the functions $\boldsymbol{\Xi}$ of equations (12*a*–12*c*). These functions have been introduced to determine the energy and entropy currents in nanosystems interacting with light. We can thus examine the impacts of these post-treatments on the laws of thermodynamics.

5.4.3. Limits. We compare three models for the interaction self-energy. Model A is the model used before any modification: the Bose–Einstein function is used, and a photon energy equal to the one of the photon source is considered for spontaneous emission (see equations (57) and (64)). Model B: the Bose–Einstein function is replaced by the number of incident photons (see equation (66)), and the photon energy for spontaneous emission is identical to the one of the photon source. Model C: the Bose–Einstein function is used, and all photon energies are considered to integrate the self-energy term of spontaneous emission (see equation (67)).

The total energy is conserved using any of the three models in the general framework of section 3, following the procedure of section 3.2.

We numerically determined the charge and entropy currents using models A, B and C, with $k_{\rm B}T_\gamma = 0.03$ eV and $k_{\rm B}T_L = 0.015$ eV; $I^e_L - V$ and $I^S - V$ characteristics are shown figure 4 ($I^e_L = -\mathrm{e}I_R$ and $I^S = \Pi$). The $I^e_L - V$ characteristics obtained using models A and B are typical of photovoltaics: the charge current is negative until the voltage reaches $V_{\rm oc}$. In the $(I^e_L \leqslant 0, V \geqslant 0)$ quadrant, the nanodevice produces electrical power, as expected from a photovoltaic device. Conversely, the charge current is already positive at zero voltage for the $I^e - V$ characteristics obtained using

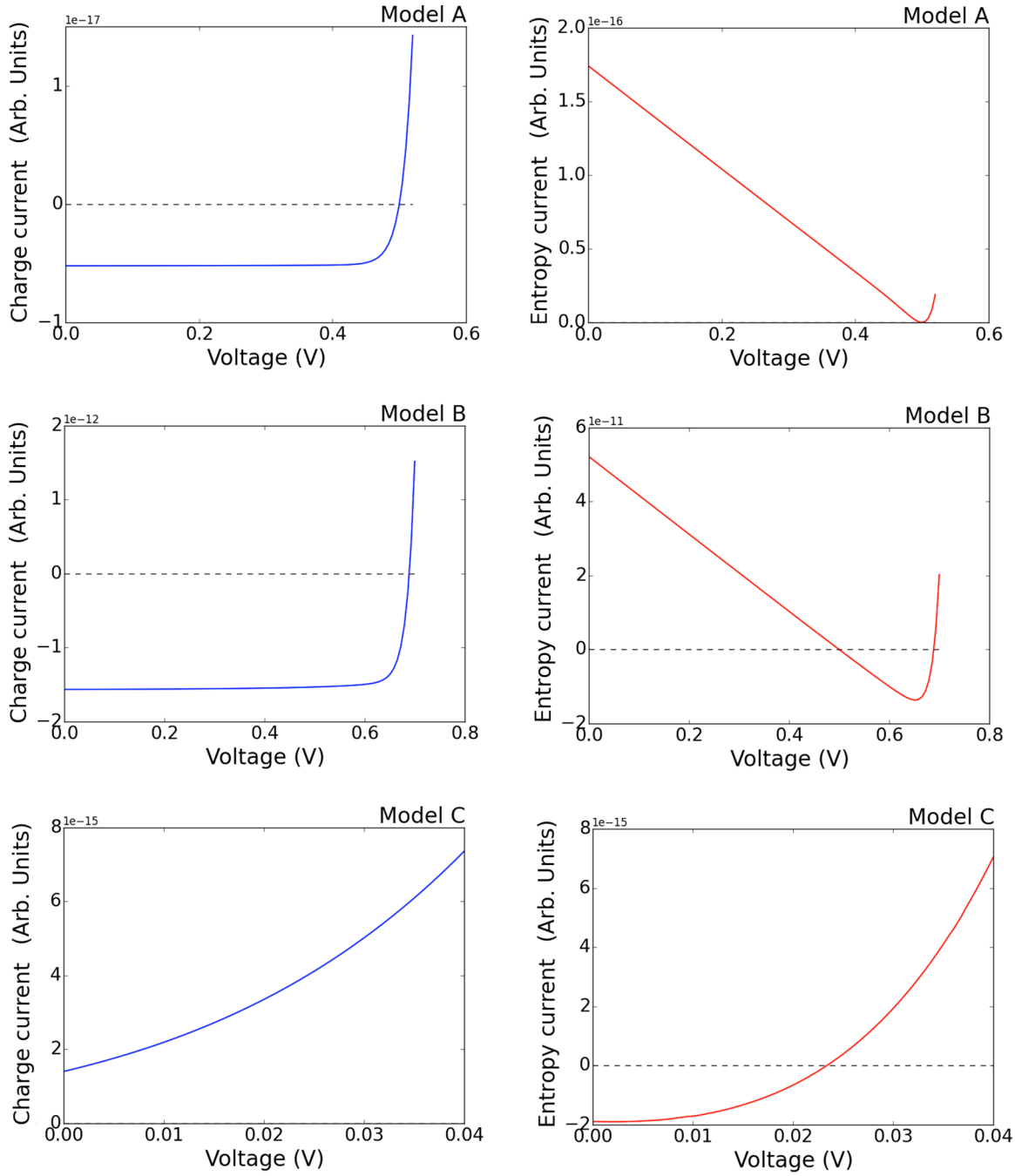

Figure 4. $I_L^e - V$ and $I^S - V$ curves in the QD-based nanojunction for the three models A, B and C detailed in the text. Differences between the $I_L^e - V$ characteristics obtained with models A and B are not significant since we have chosen a photon number close to the value of the Bose–Einstein function at $k_B T_\gamma = 0.03$ eV.

model C. The corresponding electrical power is positive: the nanodevice is consuming electrical power to produce light. That characterizes a luminescent device. The functionality of the nanodevice depends on the model choice. The $I^S - V$ curve obtained with model A exhibits a positive rate of entropy production for all voltages, as it has been proven analytically in section 5.3. Inversely, the rate of entropy production takes negative values using models B or C. Positive entropy production is no longer guaranteed using traditional post-treatments of NEGF-based simulations.

5.5. Discussion

From a fundamental viewpoint, different works show that entropy production is always positive in non-interacting nanosystems using Landauer or NEGF formalisms [11, 18, 58]. It seems still possible to show via a Landauer- *like* formulation [73] that entropy production is positive in interacting systems for which the left and right couplings to electron reservoirs are proportional. However, such a condition is not valid in photovoltaic nanodevices, since the electron/hole selectivity requires very different couplings to the left and right reservoirs. Using

NEGF formalism, light-matter interaction is included via the interaction self-energy $\mathbf{\Sigma}$, defined equation (22), and its counterparts for photons $\mathbf{\Xi}$ and $\widetilde{\mathbf{\Sigma}}$, equation (9) and equation (20) respectively, to calculate particle and energy currents in these devices. Applied to a two-level model, we demonstrated that entropy production is positive when the incident and emitted radiation have the same properties which are contained in the photon density of states (energy, polarization...). We moreover examined the impacts of two traditional modifications of the interaction self-energy which are performed after deriving particule and energy currents inside the Born approximation. Usually, the Bose Einstein function is replaced by the number of incident photons, and both induced and spontaneous radiative processes are treated independently. We showed that these two modifications no longer provide a model that guarantees a positive rate of entropy production.

Model-dependent violations of the second law of thermodynamics have already been discussed in the field of photovoltaics [74]. Actually, it would be surprising that an empirical model complies with the second law of thermodynamics. In the two critical models B and C, modifications are done after the straightforward derivation of particule and energy currents starting from the hamiltonian detailed equation (2). Models B and C can be thus regarded as empirical models. Let us reformulate the function $\mathbf{\Xi}$ of equation (9) in a general manner that includes all models:

$$\begin{aligned}\mathbf{\Xi}^{\lessgtr}_{\gamma}(\epsilon) = \sum_{\zeta\mathbf{q}\in\mathcal{M}} \hbar\omega_{\zeta\mathbf{q}}\mathbf{M}_{\zeta\mathbf{q}}[&\pm C_{abs}(\hbar\omega_{\zeta\mathbf{q}})\mathbf{G}^{\lessgtr}(\epsilon\mp\hbar\omega_{\zeta\mathbf{q}})\\ &\mp C_{em,st}(\hbar\omega_{\zeta\mathbf{q}})\mathbf{G}^{\lessgtr}(\epsilon\pm\hbar\omega_{\zeta\mathbf{q}})]\mathbf{M}_{\zeta\mathbf{q}}\\ &\mp \sum_{\zeta'\mathbf{q}'\in\mathcal{M}'} \hbar\omega_{\zeta'\mathbf{q}'}C_{em,sp}(\hbar\omega_{\zeta'\mathbf{q}'})\\ &\times \mathbf{M}_{\zeta'\mathbf{q}'}\mathbf{G}^{\lessgtr}(\epsilon\pm\hbar\omega_{\zeta'\mathbf{q}'})\mathbf{M}_{\zeta'\mathbf{q}'},\end{aligned} \tag{68}$$

where the three functions C_{abs}, $C_{em,st}$ and $C_{em,sp}$ account for each of the radiative processes (absorption, stimulated emission and spontaneous emission), and $\mathcal{M}$ and $\mathcal{M}'$ represent the two ensembles of photon modes describing the properties of the light source and the spontaneous emission respectively. From the straightforward derivation that we have presented section 3.1, one obtains a generalization of model A, characterized by: (i) the two ensembles of photon modes are identical, $\mathcal{M}=\mathcal{M}'$, (ii) $C_{abs}(\hbar\omega_{\zeta\mathbf{q}}) = C_{em,st}(\hbar\omega_{\zeta\mathbf{q}}) = N_{\zeta\mathbf{q}}$ the Bose Einstein function, and (iii) $C_{em,sp}=1$. These results directly stem from the hamiltonian model of equation (2), and from the properties of the photon Green's function $D^{0t}_{\zeta\mathbf{q}}(\tau,\tau_1) = -\mathrm{i}\langle TA_{\zeta\mathbf{q}}(t)A_{\zeta\mathbf{q}}(\tau_1)\rangle$ [43]. Functions $D^{\lessgtr}$ verify a Kubo-Martin-Schwinger relation [51]: $\mathbf{D}^{>}(\hbar\omega_{\zeta\mathbf{q}}) = \mathbf{D}^{<}(\hbar\omega_{\zeta\mathbf{q}})\mathrm{e}^{\frac{\hbar\omega_{\zeta\mathbf{q}}}{k_\mathrm{B}T_\gamma}}$, which gives the fluctuation dissipation relations $D^{>}_{\zeta\mathbf{q}} = (N_{\zeta\mathbf{q}}+1)\mathrm{Im}D^{r}_{\zeta\mathbf{q}}$ and $D^{<}_{\zeta\mathbf{q}} = N_{\zeta\mathbf{q}}\mathrm{Im}D^{r}_{\zeta\mathbf{q}}$, and the equality $N(\hbar\omega_{\zeta\mathbf{q}})+1 = \mathrm{e}^{\frac{\hbar\omega_{\zeta\mathbf{q}}}{k_\mathrm{B}T_\gamma}}N(\hbar\omega_{\zeta\mathbf{q}})$. Reciprocally, to be related to photon Green's functions, the three functions C_{abs}, $C_{em,st}$ and $C_{em,sp}$ used in equation (68) shall verify:

$$C_{em,st}(\hbar\omega_{\zeta\mathbf{q}}) + C_{em,sp}(\hbar\omega_{\zeta\mathbf{q}}) = \mathrm{e}^{\frac{\hbar\omega_{\zeta\mathbf{q}}}{k_\mathrm{B}T_\gamma}}C_{abs}(\hbar\omega_{\zeta\mathbf{q}}) \tag{69}$$

for each photon mode. Actually, models B and C do not comply with such a condition. In model B, properties (i) and (iii) are verified, but $C_{abs}(\hbar\omega_{\zeta\mathbf{q}}) = C_{em,st}(\hbar\omega_{\zeta\mathbf{q}}) = N_\phi$ a number calculated from the incoming photon source (see equation (66)). In that case, $N_\phi + 1 \neq \mathrm{e}^{\frac{\hbar\omega_{\zeta\mathbf{q}}}{k_\mathrm{B}T_\gamma}}N_\phi$. Similarly in model C, properties (ii) and (iii) are verified, but $\mathcal{M}\neq\mathcal{M}'$, which means that the two self-energy terms of induced processes and spontaneous emission are not calculated from the same photon modes. In that case again, equation (69) is not verified for each photon mode. This analysis shows that both models B and C erase the fluctuation-dissipation relations of the photon Green's functions inside the interaction self-energy, which is related to the time-reversal symmetry [75], and, hence, micro-reversibility [76].

For solar cell applications, NEGF-based simulations generally consider the whole solar spectrum. It means that the total self-energy is integrated over all photon energies. It is also possible to consider a continuous spectrum in our two-level model. The total entropy current is then calculated by integrating the analytical entropy current obtained equation (65) over all photon energies using a unique photon density of states (as in equation (67)). We thus infer that the rate of entropy production is always positive for a continuous spectrum as long as the spontaneous emission and the incident radiation are treated identically through photon properties (energy, polarization...). Nevertheless, the Bose–Einstein function shall be used. It is indeed directly related to the photon Green's function of the light source. In practice, we propose to define an equivalent temperature, T_e, from the realistic number of photons entering the absorber (see equation (66)) as $N_\phi = 1/(\exp(\hbar\omega/k_\mathrm{B}T_e)-1)$. This temperature depends on both the photon source and the absorber properties. However, for a monochromatic light source, model C still contains a contradiction: on the one hand, it may be crucial to integrate the self-energy term of spontaneous emission over all photon energies in order to determine how the device is expected to work; on the other hand, this integration results in a model which does not systematically verify the second law of thermodynamics from the entropy current expression given equation (44). This contradiction may show that incident and emitted photons no longer form a thermal reservoir in the critical range of parameters. In that case, photon temperature and chemical potential would no longer be defined. The entropy current expression of equation (44) would no longer be valid, which would explain the violation of the second law of thermodynamics. In that case, coupled Dyson's equations for both the electron and photon Green's functions would form a complete and sound model for any range of parameters.

6. Conclusion

Following the Born approximation within the Keldysh formalism, we derived the formal expressions of photon energy and particle currents in open nanosystems interacting with light. We thus obtained generalized radiation laws in terms of non-equilibrium electron Green's functions, and we found

the Planck's law at the quasi-equilibrium limit. Next, we used these expressions to formulate the spectral entropy current exchanged with the three terminals of the nanosystem, namely the two electronic reservoirs, and the photon bath. The net entropy flow was recast in the form of a difference between the efficiency of the reversible photovoltaic-thermoelectric nanodevice and its effective efficiency. We then applied these results to a two-level system illuminated with a monochromatic radiation. We showed analytically that entropy production was always positive. However, the methodology that we have presented section 3.1 is usually modified for photovoltaic applications, in order to take into account both the realistic number of photons reaching the system, and the broaden emission spectrum, notably for strong coupling to reservoirs. We found that these empirical modifications can lead to unphysical analysis since the entropy production rate can reach negative values, while energy conservation still holds. This paper provides a basic framework to discuss the ability of a quantum device to convert light energy into electrical or/and thermal energy.

Acknowledgments

We thank R Whitney, A M Daré, FGibelli, J-F Guillemoles, and LLombez for their interest in this work and for valuable discussions on different parts of this work. We acknowledge financial support from the CNRS Cellule Energie funding project 'ICARE'.

References

[1] Datta S 2009 *Electronic Transport in Mesoscopic Systems* (Cambridge: Cambridge University Press)
[2] Aeberhard U 2011 *J. Comput. Electron.* **10** 394
[3] Cavassilas N, Michelini F and Bescond M 2014 *J. Renew. Sustain. Energy* **6** 011203
[4] Marquardt F and Girvin S M 2009 *Physics* **2** 40
[5] Dubi Y and Di Ventra M 2011 *Rev. Mod. Phys.* **83** 131
[6] Benenti G, Casati G, Saito K and Whitney R S 2016 arXiv:1608.05595
[7] Stefanucci G and van Leeuwen R 2013 *Nonequilibrium Many-Body Theory of Quantum Systems: a Modern Introduction* (Cambridge: Cambridge University Press)
[8] Roy-Choudhury K and Hughes S 2015 *Phys. Rev.* B **92** 205406
[9] Wacker A 2002 *Phys. Rev.* B **66** 085326
[10] Ludovico M F, Lim J S, Moskalets M, Arrachea L and Sánchez D 2014 *Phys. Rev.* B **89** 161306
[11] Esposito M, Ochoa M A and Galperin M 2015 *Phys. Rev. Lett.* **114** 080602
[12] Crépieux A, Simkovic F, Cambon B and Michelini F 2011 *Phys. Rev.* B **83** 153417
Crépieux A, Simkovic F, Cambon B and Michelini F 2014 *Phys. Rev.* B **89** 239907
[13] Daré A M and Lombardo P 2016 *Phys. Rev.* B **93** 035303
[14] Ludovico M F, Moskalets M, Sánchez D and Arrachea L 2016 *Phys. Rev.* B **94** 035436
[15] Zhang Y, Huang C, Wang J, Lin G and Chen J 2015 *Energy* **85** 200
[16] Azema J, Daré A M, Schafer S and Lombardo P 2012 *Phys. Rev.* B **86** 075303
[17] Whitney R S 2013 *Phys. Rev.* B **87** 115404
[18] Yamamoto K and Hatano N 2015 *Phys. Rev.* E **92** 042165
[19] Benenti G and Strini G 2015 *Phys. Rev.* A **91** 020502
[20] Crépieux A and Michelini F 2015 *J. Phys.: Condens. Matter* **27** 015302
Crépieux A and Michelini F 2016 *Proc. of the UPON 2015 Conf., JSTAT p* 054015
[21] Esposito M, Ochoa M A and Galperin M 2015 *Phys. Rev.* B **91** 115417
[22] Henrickson L E 2002 *J. Appl. Phys.* **91** 6273
[23] Aeberhard U and Morf R H 2008 *Phys. Rev.* B **77** 125343
[24] Cavassilas N, Gelly C, Michelini F and Bescond M 2015 *IEEE J. Photovolt.* **5** 1621
[25] Beltako K, Cavassilas N and Michelini F 2016 *Appl. Phys. Lett.* **109** 073501
[26] Park K T *et al* 2013 *Sci. Rep.* **3** 2123
[27] BjØrk R and Nielsen K K 2015 *Sol. Energy* **120** 187
[28] Even J *et al* 2015 *J. Phys. Chem.* C **119** 10161
[29] Mettan X *et al* 2015 *J. Phys. Chem.* C **119** 11506
[30] Ning Z *et al* 2015 *Nature* **523** 324
[31] Rey M, Strass M, Kohler S, Hänggi P and Sols F 2007 *Phys. Rev.* **76** 085337
[32] Cleuren B, Rutten B and Van den Broeck C 2012 *Phys. Rev. Lett.* **108** 120603
[33] Mari A and Eisert J 2012 *Phys. Rev. Lett.* **108** 120602
[34] Wang J, Lai Y, Ye Z, He J, Ma Y and Liao Q 2015 *Phys. Rev.* E **91** 050102
[35] Entin-Wohlman O, Imry Y and Aharony A 2015 *Phys. Rev.* B **91** 054302
[36] Markvart T 2016 *WIREs Energy Environ* (https://doi.org/10.1002/wene.204)
[37] Würfel P 2009 *Physics of Solar Cells* (New York: Wiley)
[38] Humphrey T E and Linke H 2005 *Phys. Rev. Lett.* **94** 096601
[39] Rodière J, Lombez L, Le Corre A, Durand O and Guillemoles J F 2015 *Appl. Phys. Lett.* **106** 183901
[40] Campisi M and Fazio R 2016 *Nat. Commun.* **7** 11895
[41] Mandel L and Wolf E 1995 *Optical Coherence and Quantum Optics* (Cambridge: Cambridge University Press)
[42] Haug H and Jauho A P 2008 *Quantum Kinetics in Transport and Optics of Semiconductors* (Berlin: Springer)
[43] Mahan G D 2000 *Many-Particle Physics* 3rd edn (Dordrecht: Kluwer)
[44] Baym G and Kadanoff L P 1961 *Phys. Rev.* **124** 287
Baym G 1962 *Phys. Rev.* **127** 139
[45] Aeberhard U 2011 *Phys. Rev.* B **84** 035454
[46] Richter F, Florian M and Henneberger K 2008 *Phys. Rev.* B **78** 205114
[47] Fetter A L and Walecka J D 1971 *Quantum Theory of Many-Particle Systems* (New York: McGaw-Hill)
[48] Meair J, Bergfield J P, Stafford C A and Jacquod P 2014 *Phys. Rev.* B **90** 035407
[49] Whitney R S, Sánchez R, Haupt F and Splettstoesser J 2016 *Physica* E **75** 257
[50] Bruus H and Flensberg K 2004 *Many-body Quantum Theory in Condensed Matter Physics* (New York: Oxford University Press)
[51] Balzer K and Bonitz M 2013 *Nonequilibrium Green's Functions Approach to Inhomogeneous Systems* (Berlin: Springer)
[52] Würfel P 1982 *J. Phys. C: Solid State Phys.* **15** 3967–85
[53] Lasher G and Stern F 1964 *Phys. Rev.* **133** A553
[54] Berbezier A and Aeberhard U 2015 *Phys. Rev. Appl.* **4** 044008
[55] Gibelli F, Lombez L, Rodière J and Guillemoles J F 2016 *Phys. Rev. Appl.* **5** 024005
[56] Esposito M and Van den Broeck C 2010 *Phys. Rev.* E **82** 011143
[57] Einax M, Dierl M and Nitzan A 2011 *Phys. Chem.* C **115** 21396–401
[58] Whitney R S 2015 *Phys. Rev.* B **91** 115425
[59] Landsberg P T and Badescu V 1998 *Prog. Quantum Electron.* **22** 211

[60] Green M 2005 *Third Generation Photovoltaics: Advanced Solar Energy Conversion* (Berlin: Springer)
[61] Rutten B, Esposito M and Cleuren B 2009 *Phys. Rev.* B **80** 235122
[62] Ruokola T and Ojanen T 2012 *Phys. Rev.* B **86** 035454
[63] Sánchez R and Büttiker M 2012 *Europhys. Lett.* **100** 47008
[64] Jordan A N, Sothmann B, Sánchez R and Büttiker M 2013 *Phys. Rev.* B **87** 075312
[65] Argawalla B K and Segal D 2016 *J. Chem. Phys.* **144** 074102
[66] Sánchez R and Buttiker M 2011 *Phys. Rev.* B **83** 085428
[67] Thierschmann H, Sánchez R, Sothmann B, Arnold F, Hyen C, Hansen W, Buhmann H and Molenkamp L W 2015 *Nat. Nanotechnol.* **10** 854
[68] Jauho A P, Wingreen N S and Meir Y 1994 *Phys. Rev.* B **50** 5528
[69] Entin-Wohlman O, Jiang J H and Imry Y 2014 *Phys. Rev.* E **89** 012123
[70] Berbezier A, Autran J L and Michelini F 2013 *Appl. Phys. Lett.* **103** 041113
[71] Zamoum R, Lavagna M and Crépieux A 2016 *Phys. Rev.* B **93** 235449
[72] Steiger S 2009 *PhD Thesis ETH* Zurich
[73] Meir Y and Wingreen N S 1992 *Phys. Rev. Lett.* **68** 2512
[74] Luque A and Martí A 1997 *Phys. Rev.* B **55** 6994
[75] Whitney R S 2016 arXiv:1611.00670
[76] Campisi M, Hänggi P and Talkner P 2011 *Rev. Mod. Phys.* **83** 771